Phase Polymorphism of $[Ni(DMSO)_6](ClO_4)_2$ Studied by Differential Scanning Calorimetry

Anna Migdał-Mikuli and Elżbieta Szostak

Department of Chemical Physics, Faculty of Chemistry, Jagiellonian University, ulica Ingardena 3, 30-060 Kraków, Poland

Reprint requests to Dr. hab. A. M.-M.; Fax: +48-12-634-0515; E-mail: migdalmi@chemia.uj.edu.pl

Z. Naturforsch. **62a,** 67 – 74 (2007); received September 18, 2006

Six solid phases of $[Ni(DMSO)_6](ClO_4)_2$ have been detected by differential scanning calorimetry (DSC). The five phase transitions were detected between the following solid phases: metastable KIII ↔ undercooled K0 at T_{C5} = 326 K, stable KIb → stable KIa at T_{C4} = 350 K, metastable KII ↔ undercooled KI at T_{C3} = 353 K, stable KIa → stable KI at T_{C2} = 365 K and stable KI → stable K0 at T_{C1} = 380 K. At T_{m2} = 459 K the title compound partially dissolves in DMSO, which arises from the decomposition of $[Ni(DMSO)_6](ClO_4)_2$ to $[Ni(DMSO)_5](ClO_4)_2$, and at T_{m1} = 526 K created in this way a substance which completely melts. From the entropy changes at the melting point and at phase transitions it can be concluded that the phases K0 and undercooled K0 are orientationally dynamically disordered crystals. The stable phases KI, KIa, KIb and the metastable phases KII and KIII are more or less ordered solids.

Key words: Hexadimethylsulphoxidenickel(II) Chlorate(VII); Phase Transitions; Melting Point; DSC.

1. Introduction

HNiC, i. e. $[Ni(DMSO)_6](ClO_4)_2$, where DMSO is dimethylsulphoxide, crystallizes in a trigonal system at room in ambient temperature and belongs to the $P31c$ space group (No. 159) [1]. These crystals form a primitive lattice with two molecules in an unit cell. The lattice parameters are: a = 11.819 Å and c = 12.361 Å [1]. HNiC contains two kinds of ions: $[Ni((CH_3)_2SO)_6]^{2+}$ and ClO_4^-. The cation is a slightly deformed octahedron, where Ni is surrounded by six oxygen atoms coming from the DMSO ligands, which are built like C_{2v} pyramids. We have recently investigated the polymorphism of HCoC and HZnC, i. e. $[Co(DMSO)_6](ClO_4)_2$ and $[Zn(DMSO)_6](ClO_4)_2$, using differential scanning calorimetry (DSC) [2, 3]. These compounds are isostructural with HNiC. We have found that HCoC has five and HZnC has four solid phases. Two and one of them, respectively, are (is) metastable, and the other ones are stable. The high temperature phases of these compounds can be easily undercooled. The purpose of the present work was to check carefully the polymorphism of HNiC in the temperature range of 93 – 530 K, using DSC.

2. Experimental

2.1. Sample Preparation

A few grams of $[Ni(H_2O)_6](ClO_4)_2$ were dissolved while being slowly heated in DMSO of high chemical purity [4], which was previously additionally purified by vacuum distillation at low pressure. This solution was then chilled, and the precipitated crystals of HNiC were filtered and washed with acetone. The crystals were dried in a desiccator over phosphorous pentaoxide for a few hours. After desiccation, they were put in a sealed vessel and stored in a desiccator with barium oxide as a desiccant.

To check the chemical composition of the synthesized HNiC, the percentage content of nickel ions was checked using a complexometric method, with a solution of the sodium salt of ethylenediaminetetraacetic acid (EDTA) as a titrant. The content of carbon and hydrogen in the DMSO ligand was determined using elementary analysis in an EURO EA 3000 apparatus. The theoretical content of nickel equalled 8.08%, and its content found by titration analysis amounted to (7.98 ± 0.12)%. For the carbon atoms, the differ-

Table 1. Band positions of the Raman and infrared spectra of solid $[Ni(DMSO)_6](ClO_4)_2$ and liquid DMSO at room temperature (frequencies in cm^{-1}).

vw, very weak; w, weak; sh, shoulder; m, medium; st, strong; vst, very strong; br, broad.

$[Ni(DMSO)_6](ClO_4)_2$				DMSO		
RS	IR			RS	IR	
This work	This work in KBr pellet	This work [a] in Apiezon [b] in Nujol	Literature [5, 6]	Literature [7, 8]		Assignment
		58 w[a]	61 w			ν_L(lattice)
		74 w[a]	74 sh			ν_L(lattice)
108 vw		97 m[a]	98 m			ν_d(NiO)
131 sh		132 m[a]	132 m			ν_s(NiO)
189 vw		187 m[a]	186 m			δ_d(NiOS)
206 sh						ν_d(NiO)
250 vw		244 st,br[a]	243 st,br			ν_s(NiO)
316 m		322 st[a]	318 st	313 m	313 w	δ_{as}(CSC)
343 m		349 st[a]	344 st	338 m	338 m	δ_{as}(CSO)
		381 w[a]		388 m	381 m	δ_s(CSO)
424 w						ν_s(NiO)
		446 m[a]	444 m			ν_s(NiO)
458 w	458 w					δ_d(OClO) E
625 w	628 st	624 st[b]				δ_d(OClO) F_2
					612 sh	ν_s(CS)
681 vst	668 w	681 w[b]		663 vst	663 m	ν_s(CS)
716 st	713 m	716 m[b]	716 w	700 m	700 st	ν_{as}(CS)
911 w	907 vw	904 sh		900 vw	900 w	$\rho(CH_3)$
934 vst						ν_s(ClO) A_1
	938 sh	941 st[b]		925 vw	931 m	$\rho(CH_3)$
954 w	953 st	953 st[b]		954 w	955 st	$\rho(CH_3)$
1002 w						$\rho(CH_3)$
		999 st[b]	1002 sh			ν_s(SO)
1017 w	1016 vst	1026 sh[b]				ν_s(SO)
1036 w				1050 m	1050 vst	ν_s(SO)
1099 vw	1097 st	1093 st[b]				ν_d(ClO) F_2
	1114 st					
	1299 sh	1299 w[b]			1303 m	δ_s(HCH)
	1317 m	1318 m[b]		1313 w		δ_s(HCH)
		1377 m[b]				δ_{as}(HCH)
	1407 m	1409 sh[b]			1404 st	δ_{as}(HCH)
1421 st	1418 m	1418 m[b]				δ_{as}(HCH)
	1435 m	1443 vst[b]		1425 m	1440 st	δ_{as}(HCH)
		1457 vst[b]				δ_{as}(HCH)
	2851 w	2852 vst[b]		2885 br	2825 br	ν_s(CH)
		2870 sh[b]				ν_s(CH)
2922 vst	2916 w	2916 vst[b]		2913 vst	2910 st	ν_s(CH)
		2955 vst[b]				ν_{as}(CH)
3009 st	3002 w	3004 st[b]		2999 m	2999 st	ν_{as}(CH)
3226 br						

ence between the theoretical (19.84%) and test value [(19.90 ± 0.01)%] did not exceed 0.1%. For the hydrogen atoms, the theoretical value was 5.00% and the test value (4.74 ± 0.01)%. Therefore, the elementary analysis of the title compound confirmed the presence of the stoichiometric number of six DMSO molecules in the complex cation.

2.2. Sample Characteristics

For further identification of the title compound, its infrared absorption spectra (FT-FIR and FT-MIR) and its Raman spectrum (FT-RS) were recorded at ambient temperature. The FT-FIR and FT-MIR spectra were made using Digilab FTS-14 and EQUINOX-55 Bruker Fourier transform infrared spectrometers, respectively, with a resolution of 2 cm^{-1}. The FT-FIR spectrum for powder samples, suspended in Apiezon grease, was recorded. Polyethylene and silicon windows were used. The FT-MIR spectrum was recorded for a sample suspended in Nujol between the KBr pellets. The FT-RS spectrum was recorded using a Bio-Rad spectrometer with a YAG neodymium laser (λ = 1064 nm) at 10 – 4000 cm^{-1} with a resolution

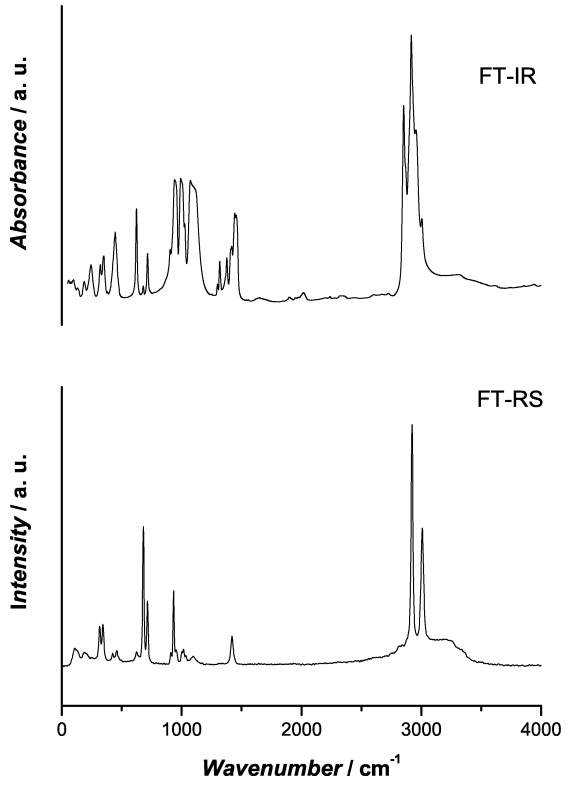

Fig. 1. Comparison of the infrared (FT-IR) and Raman (FT-RS) spectra of HNiC.

of 4 cm^{-1}. Figure 1 presents a comparison of the infrared and Raman spectra of HNiC. Table 1 contains a list of the obtained and literature data [5 – 8] of band frequencies and their assignments. The recorded spectra additionally identify the investigated compound as $[Ni(DMSO)_6](ClO_4)_2$.

Thermal analysis of the examined compound was made in order to further verify its composition. The differential thermal analysis (DTA) and thermogravimetry (TG) measurements were performed using a Mettler Toledo TGA/SDTA 851^e apparatus. A sample weighing 15.8375 mg was placed in a 150 µl corundum crucible. The thermogravimetric measurements were made in a flow of argon (80 ml/min) from 300 up to 670 K at a constant heating rate of 10 $K \cdot min^{-1}$. The temperature was measured by a Pt-Pt/Rh thermocouple with an accuracy of ±0.5 K. The TG measurements of HNiC proved that during the heating of a sample from 300 up to 400 K (in a flow of argon) the sample does not lose more than ca. 3% of its initial mass. During heating up to 470 K the sample loses 10.23% of its initial mass and converts into $[Ni(DMSO)_5](ClO_4)_2$.

Table 2. Thermodynamics parameters of the detected phase transitions (on heating, T^h, and cooling, T^c) in $[Ni(DMSO)_6](ClO_4)_2$.

	T_c [K]	ΔH [$kJ \cdot mol^{-1}$]	ΔS [$J \cdot mol^{-1} \cdot K^{-1}$]
T^h_{m1} *	526 ± 2	–	–
T^h_{m2}	459 ± 1	3.98 ± 0.12	8.7 ± 0.3
T^h_{C1}	380 ± 2	24.18 ± 0.53	63.7 ± 1.2
T^h_{C2}	365 ± 1	7.72 ± 0.17	21.2 ± 0.5
T^h_{C3}	353 ± 1	1.60 ± 0.07	4.5 ± 0.2
T^h_{C4}	350 ± 1	0.38 ± 0.04	1.1 ± 0.1
T^c_{C5}	326 ± 1	27.54 ± 0.26	84.4 ± 0.8

* Melting of $[Ni(DMSO)_5](ClO_4)_2$ under DMSO vapour pressure.

To sum up, the FT-RS, FT-FIR, and FT-MIR spectra, and chemical and thermal analyses (TG + QMS and SDTA) have jointly certified the composition and purity of the examined compound.

2.3. Heat Flow Measurements

The DSC measurements of HNiC were made using two types of DSC apparatus: the first one was a Perkin-Elmer PYRIS 1 DSC apparatus used in the temperature range of 93 – 423 K for sample hermetically closed in 30 µl aluminium containers. The weight of that sample was 15.64 mg (sample *a*). The second one was a Mettler Toledo DSC 821e apparatus used in the temperature range of 253 – 530 K. The weight of the sample *b* was 9.61 mg. The details of the DSC experiment were the same as described in [9, 10].

3. Results and Discussion

Temperature dependences of the difference in thermal power supplied to the two calorimeters (the so-called thermal stream or heat flow), named DSC curves, were obtained for each of two HNiC samples *a* and *b* at different scanning rates and at different initial and final sample heating and cooling conditions. Different masses of the samples were chosen in order to determine whether the observed phase transition depends on the sample weight, or not. We did not notice significant differences between the results obtained for the samples *a* and *b*, so we will present only the results for sample *b*. The thermodynamics parameters of the detected phase transitions are presented in Table 2. The results of all DSC measurements are also schematically presented as a temperature dependence of the free enthalpy *G* (Gibbs free energy) in Figure 2.

Samples of a crystalline phase without any "thermal history" are called KIb phase. The measurements

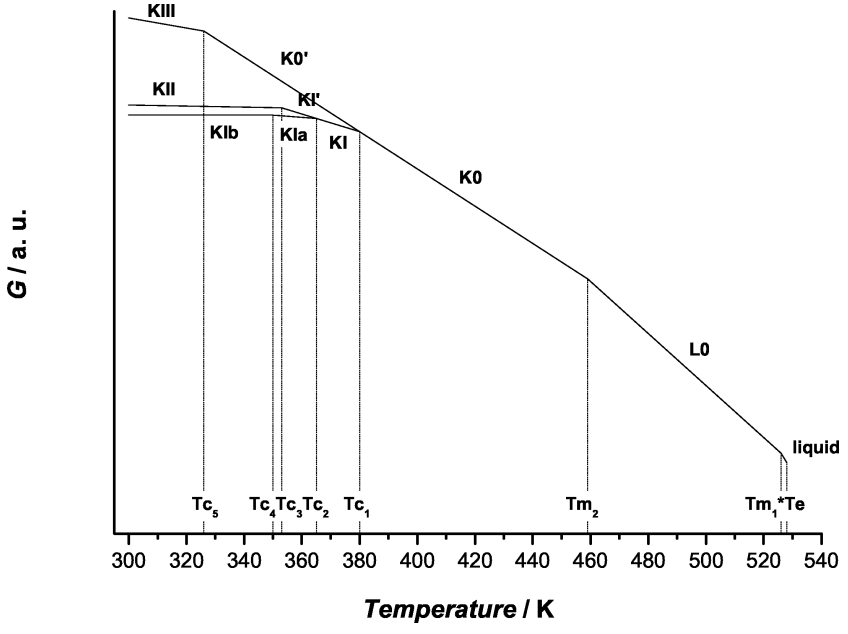

Fig. 2. Scheme of temperature dependence of the free enthalpy G of HNiC. $T_{m1}{}^*$, melting point of $[Ni(DMSO)_5](ClO_4)_2$ under DMSO vapour pressure.

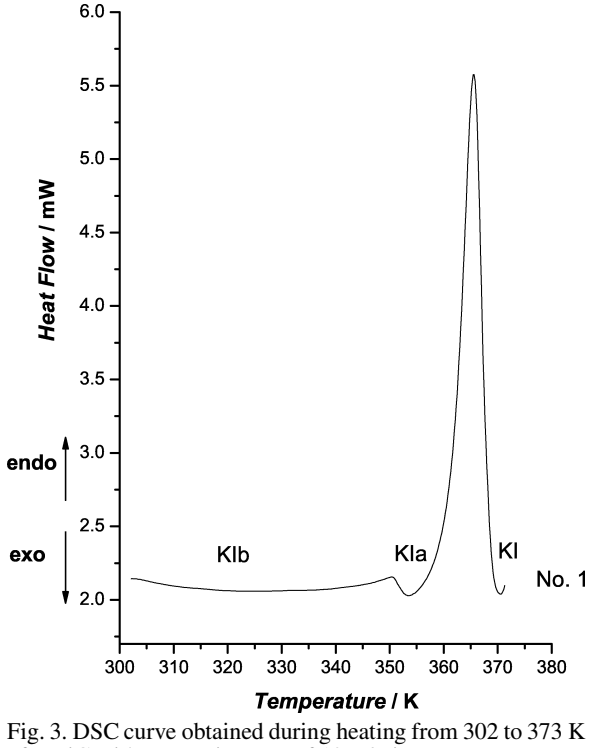

Fig. 3. DSC curve obtained during heating from 302 to 373 K of HNiC with a scanning rate of 10 K/min.

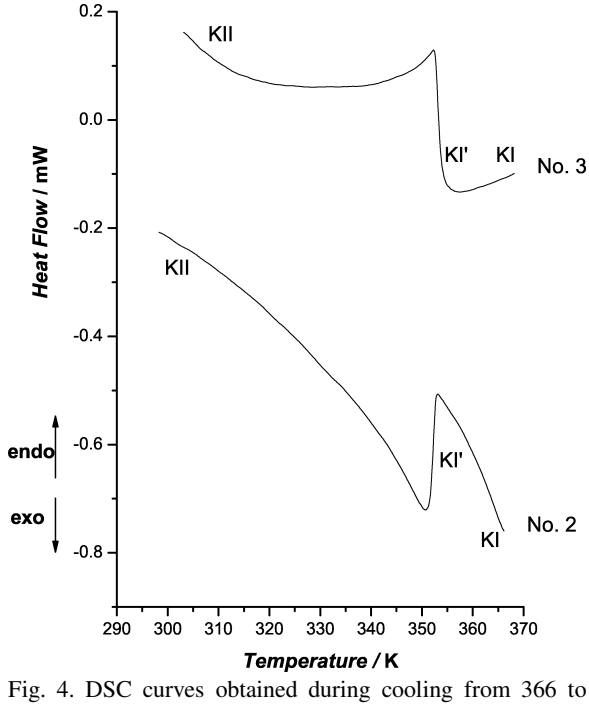

Fig. 4. DSC curves obtained during cooling from 366 to 298 K (curve No. 2) and during heating at 303 – 369 K (curve No. 3) of HNiC with a scanning rate of 10 K/min.

on sample *a* were started by cooling the sample from room temperature to 93 K, holding it at this temperature for 1 minute, then heating the sample to 298 K.

There was no anomaly of the DSC curve obtained at first cooling and subsequent heating the sample *a* with a scanning rate of 40 K/min; therefore these curves are not presented here.

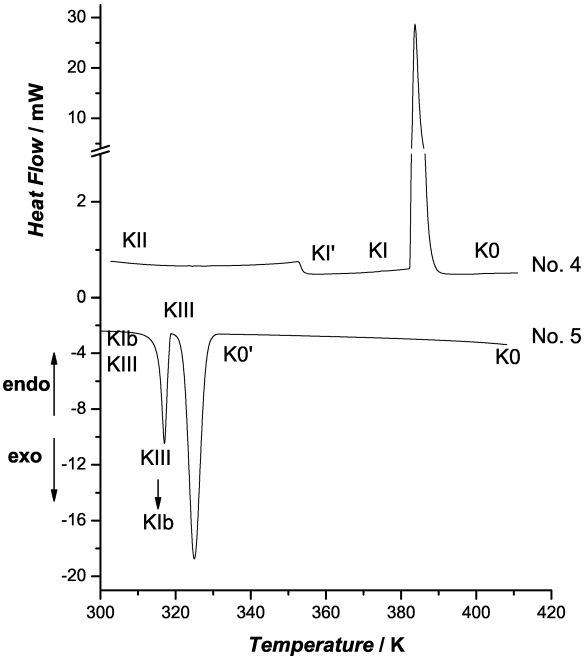

Fig. 5. DSC curves obtained during heating from 300 to 410 K (curve No. 4) and during cooling at 418 – 300 K (curve No. 5) of HNiC with a scanning rate of 10 K/min.

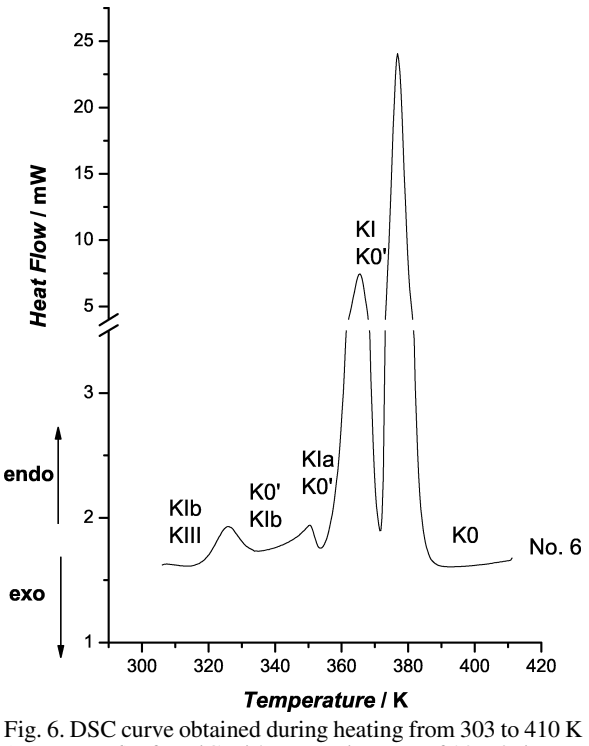

Fig. 6. DSC curve obtained during heating from 303 to 410 K (curve No. 6) of HNiC with a scanning rate of 20 K/min.

While heating sample *b*, being initially in the KIb phase, from room temperature RT to 373 K, a phase transition into an intermediate phase, which is named KIa, is observed at T^{h}_{C4} = 350 K, which is manifested in a small anomaly on the DSC curve No. 1 (Fig. 3). Phase KIa next transforms into the phase KI at T^{h}_{C2} = 365 K, which is manifested by a relatively big anomaly on the same curve (see Fig. 3 and compare with Fig. 2).

While cooling sample *b* in the KI phase from 373 to 298 K, a slight undercooling is observed. The undercooled phase KI passes the metastable phase KII at T^{h}_{C3} = 353 K. The transition from the undercooled KI phase to the KII phase (at T^{h}_{C2}) is reversible. This is clearly visible in Fig. 4, showing DSC curves that were recorded during cooling (curve No. 2) and heating (curve No. 3) of sample *b* in the temperature range of 366 – 298 K with a rate of 10 K/min. Both during heating and cooling the sample, a small anomaly on the DSC curves was detected that is due to a phase transition: undercooled KI phase ↔ KII phase.

Heating of sample *b* with a scanning rate of 10 K/min in the temperature range of 300 – 410 K gives the DSC curve No. 4, on which we can see one small anomaly at T^{h}_{C3}, connected with the phase transition "metastable phase KII ↔ undercooled phase KI" and one major anomaly at T^{h}_{C1}, connected with the phase transition "stable phase KI → stable phase K0".

Later, while cooling the sample from 410 K with a scanning rate of 10 K/min, being in the K0 phase, undergoes a deep undercooling. As can be seen in Fig. 5 (DSC curve No. 5), when the sample is cooled, the undercooled K0 phase experiences a phase transition at T^{h}_{C5} = 326 K into a metastable phase, called KIII phase, which is connected with a big anomaly on the DSC curve. On further cooling, at ca. 317 K the KIII phase undergoes a spontaneous transformation partially into the stable phase KIb, which is manifested in a relatively big anomaly on the DSC curve (ΔH = 7.50 kJ/mol).

New heating of sample *b* with a scanning rate of 20 K/min gives the DSC curve No. 6 presented in Figure 6. The part of the sample in the metastable phase KIII transforms by an endothermic process into the undercooled phase K0 at 326 K (small and broad anomaly on the DSC curve). When the heating of the sample is continued, the phase transition occurs from phase KIb to KIa at T^{h}_{C4} (small but sharp endothermic anomaly) and, at a slightly higher temperature, phase KIa transforms to phase KI (big and broad endothermic anomaly

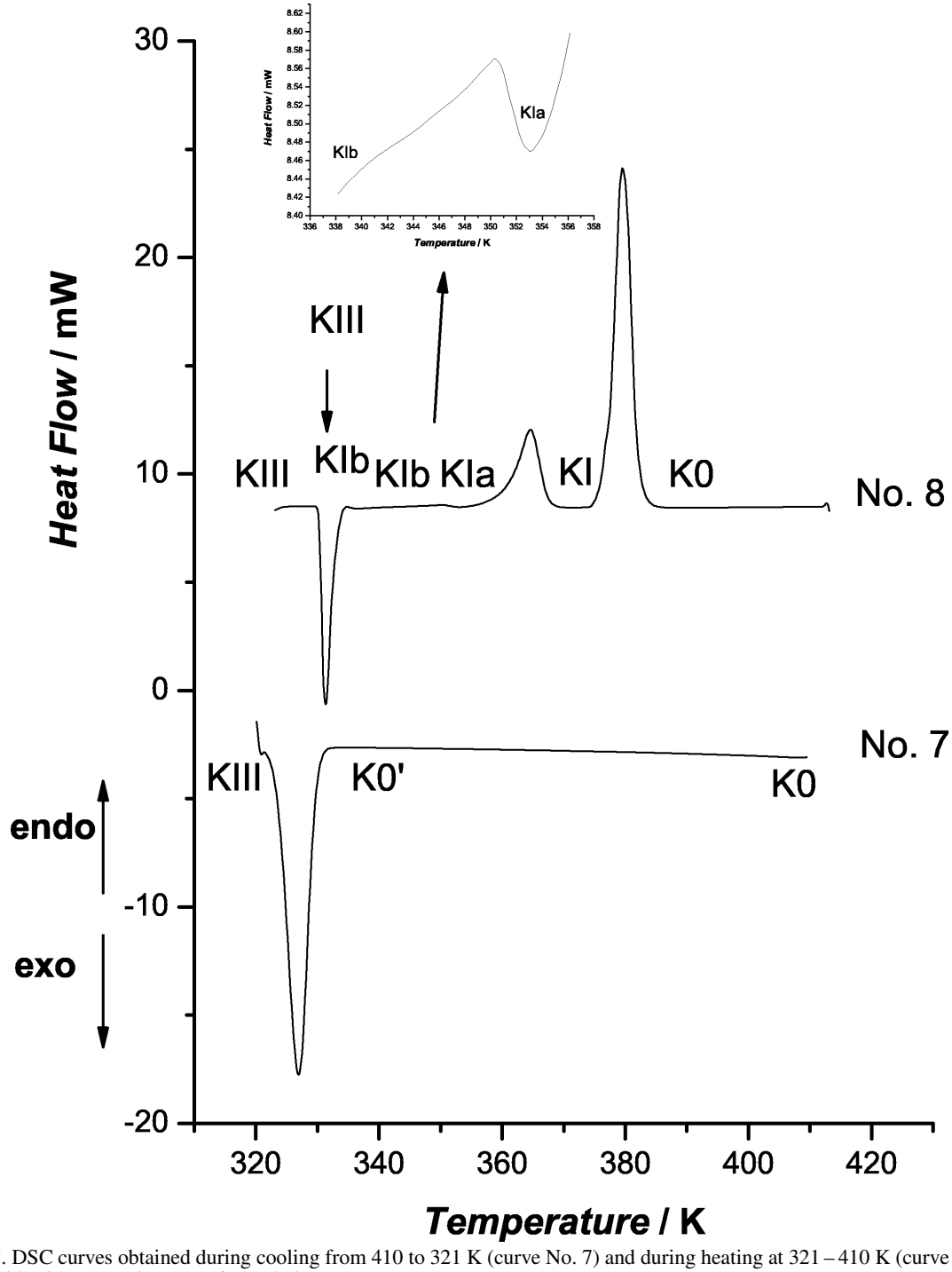

Fig. 7. DSC curves obtained during cooling from 410 to 321 K (curve No. 7) and during heating at 321 – 410 K (curve No. 8) of HNiC with a scanning rate of 10 K/min.

at T_{C2}^{h}). Finally, the stable phase KI also endothermically converts at T_{C1}^{h} to phase K0 (very big anomaly on the DSC curve No. 6). All these transitions can also be identified on the scheme presented in Figure 2.

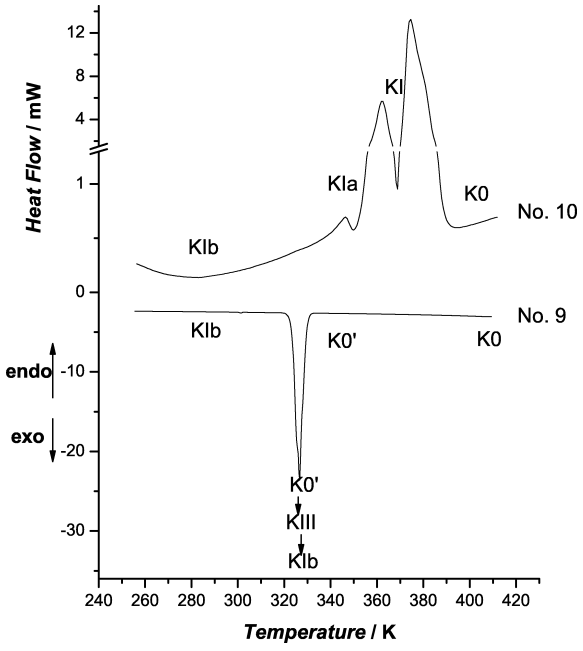

Fig. 8. DSC curves obtained during cooling from 410 to 253 K (curve No. 9) and during heating at 255 – 410 K (curve No. 10) of HNiC with a scanning rate of 20 K/min and 40 K/min, respectively.

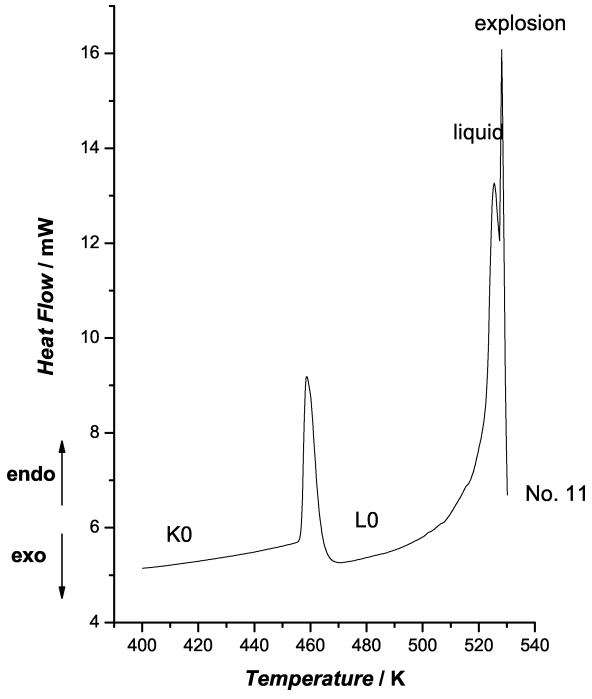

Fig. 9. DSC curve obtained in the temperature range of 400 – 530 K during heating of HNiC with a scanning rate of 20 K/min.

To prove that phase KIII is metastable sample *b* was cooled from 410 K to 321 K with a scanning rate of 10 K/min. As shown in Fig. 7 (DSC curve No. 7), in this temperature range we can see only a phase transition connected with the transformation of the undercooled phase K0 to the metastable phase KIII. When the same sample is heated up (DSC curve No. 8), the metastable phase KIII, at ca. 340 K, undergoes a spontaneous conversion phase KIb, which is manifested by a relatively big and sharp exothermic anomaly on the DSC curve. We believe that this process is similar to crystallisation of a new phase [11]. When the heating of the sample is continued, the phase transition occurs from phase KIb to KIa at T^{h}_{C4} (very small and broad endothermic anomaly) and, at a slightly higher temperature, the phase KIa converts endothermically to the phase KI (big and broad anomaly at T^{h}_{C2}). Later, the stable phase KI also endothermically converts at T^{h}_{C1} to the stable phase K0 (very big anomaly on the DSC curve No. 8).

The cooling of sample *b* in the temperature range of 410 – 253 K with a scanning rate of 20 K/min gives a somewhat different picture of the phase transformation, which can be seen on the DSC curves presented in Figure 8. While the sample being in the K0 phase is cooled from 410 K, it becomes undercooled. As shown in Fig. 8 (DSC curve No. 9), while being cooled, the undercooled K0 phase converts into the metastable phase KIII and undergoes a spontaneous conversion into the stable phase KIb simultaneously, which is manifested in a very big anomaly. It should be stressed that the change of the enthalpy of this transition ΔH = 35.38 kJ/mol is the sum of enthalpies connected with the phase transition, the undercooled phase K0, the metastable phase KIII, and with the conversion of the metastable phase KIII into the stable phase KIb.

The heating of this sample with the scanning rate 40 K/min stimulates the phase transition from the stable phase KIb to the stable phase KIa at T^{h}_{C4} (sharp endothermic anomaly on the DSC curve No. 10 in Fig. 8) and then the stable phase KIa converts into the stable phase KI (relatively big endothermic anomaly at T^{h}_{C2}). At the end, the stable phase KI endothermically converts at T^{h}_{C1} into the stable phase K0 (big and broad anomaly on the DSC curve).

Using a microscope it was observed that all the five detected phases were solid phases, and the phase denoted by L0 in Fig. 9 is a partly melted phase. Taking into account the results of the thermal anal-

ysis, we can postulate that at T_{m2} = 459 K the sample partly dissolves in DMSO, which arises because of the decomposition of $[Ni(DMSO)_6](ClO_4)_2$ to $[Ni(DMSO)_5](ClO_4)_2$. This dissolving is possible because the sample is hermetically closed in the calorimeter during our DSC experiment. Thus this phase transition is reversible and is the reason that during the heating the sample melts in a two-stage process, first partly at T_{m2} = 459 K with ΔH_{m2} = 3.98 kJ/mol and then completely at T_{m1} = 525 K. It was concluded from the change of the entropy of transition ΔS (see Table 2) that the phases K0 and undercooled K0 are more likely to be orientationally dynamically disordered crystals, the so-called "ODDIC". The phases KI, KIa, KIb, KII and KIII are more or less ordered ones (very big values of ΔS connected with the KIII ↔ K0 and KI ↔ K0 phase transitions at T^h_{C5} and T^h_{C1}, respectively, and small values of ΔS connected with the phase transitions KIb ↔ KIa, KIa ↔ KI, and KII ↔ KI', see Table 2.).

The sample above 530 K becomes unstable and explodes at T_e. That is why we had to finish the heating of the sample just after it completely melt. A DSC curve showing the anomalies resulting from the two-stage melting process of the title compound is shown in Figure 9. A two-stage melting connected with a partial dehydratation of the sample was observed by us also in the case of $[Ni(H_2O)_6](NO_3)_2$ [12].

4. Conclusions

1. The following phase transitions of HNiC have been discovered and thermodynamics parameters have been determined:

- total melting of the sample under DMSO vapour pressure at T_{m1} = 526 K;
- partial melting of the crystals – the transition: stable phase K0 ↔ stable phase L0 (the partially melted phase K0) at T_{m2} = 459 K with ΔS = 8.7 J · mol^{-1} · K^{-1};
- irreversible transition: stable phase KI ↔ stable phase K0 at T^h_{C1} = 380 K with ΔS = 63.7 J · mol^{-1} · K^{-1};
- irreversible transition: stable phase KIa ↔ stable phase KI at T^h_{C2} = 365 K with ΔS = 21.2 J · mol^{-1} · K^{-1};
- reversible transition: metastable phase KII ↔ undercooled phase KI at T^h_{C3} = 353 K with ΔS = 4.5 J · mol^{-1} · K^{-1};
- irreversible transition: stable phase KIb ↔ stable phase KIa at T^h_{C4} = 350 K with ΔS = 1.1 J · mol^{-1} · K^{-1};
- reversible transition: metastable phase KIII ↔ undercooled phase K0 at T^h_{C5} = 326 K with ΔS = 84.4 J · mol^{-1} · K^{-1}.

2. It can be concluded from the small entropy changes on melting that the phases K0 and undercooled K0 are so-called "orientationally dynamically disordered crystals" (ODDIC). Phases KI, KIa, KIb, KII and KIII are more or less ordered phases.

Acknowledgements

We thank Dr. hab. E. Mikuli from our faculty for stimulating discussions and Dr. C. Paluszkiewicz and Dr. hab. A. Wesełucha-Birczyńska from the Regional Laboratory of Physicochemical Analysis and Structural Research in Kraków for help in recording the FT-FIR and FT-RS spectra.

[1] E. J. Chan, B. G. Cox, J. M. Harrowfield, M. I. Ogden, B. W. Skelton, and A. H. White, Inorg. Chim. Acta **357**, 2365 (2004).
[2] A. Migdał-Mikuli and E. Szostak, Thermochim. Acta **426**, 191 (2005).
[3] A. Migdał-Mikuli and E. Szostak, Thermochim. Acta **444**, 195 (2006).
[4] F. A. Cotton and R. Francis, J. Am. Chem. Soc. **82** 2986 (1960).
[5] D. M. Adams and W. R. Trumble, Inorg. Chem. **15**, 1968 (1976).
[6] J. Selbin, W. E. Bull, and L. H. Holmes Jr., J. Inorg. Nucl. Chem. **16**, 219 (1961).
[7] Raman/IR Atlas, Verlag Chemie GmbH, Weinheim 1974.
[8] K. Nakamoto, Infrared and Raman Spectra of Inorganic and Coordination Compounds, Part B, 5th ed., A. Wiley Intersience Publ., New York 1997.
[9] A. Migdał-Mikuli, E. Mikuli, S. Wróbel, and Ł. Hetmańczyk, Z. Naturforsch. **54a**, 590 (1999).
[10] E. Mikuli, A. Migdał-Mikuli, M. Liszka, and M. Molenda, J. Therm. Anal. Calorim. (2006); DOI: 10.1007/510973-006-7610-6.
[11] Y. Mnyukh, Fundamentals of Solid-State Phase Transitions, Ferromagnetism and Ferroelectricity, 1st Books Library, Bloomington 2001.
[12] E. Mikuli, A. Migdal-Mikuli, R. Chyży, B. Grad, and R. Dziembaj, Thermochim. Acta **370**, 65 (2001).